

AIParsing: Anchor-free Instance-level Human Parsing

Sanyi Zhang, *Member, IEEE*, Xiaochun Cao, *Senior Member, IEEE*, Guo-Jun Qi, *Fellow, IEEE*, Zhanjie Song, *Member, IEEE*, and Jie Zhou, *Senior Member, IEEE*

Abstract—Most state-of-the-art instance-level human parsing models adopt two-stage anchor-based detectors and, therefore, cannot avoid the heuristic anchor box design and the lack of analysis on a pixel level. To address these two issues, we have designed an instance-level human parsing network which is anchor-free and solvable on a pixel level. It consists of two simple sub-networks: an anchor-free detection head for bounding box predictions and an edge-guided parsing head for human segmentation. The anchor-free detector head inherits the pixel-like merits and effectively avoids the sensitivity of hyper-parameters as proved in object detection applications. By introducing the part-aware boundary clue, the edge-guided parsing head is capable to distinguish adjacent human parts from among each other up to 58 parts in a single human instance, even overlapping instances. Meanwhile, a refinement head integrating box-level score and part-level parsing quality is exploited to improve the quality of the parsing results. Experiments on two multiple human parsing datasets (*i.e.*, CIHP and LV-MHP-v2.0) and one video instance-level human parsing dataset (*i.e.*, VIP) show that our method achieves the best global-level and instance-level performance over state-of-the-art one-stage top-down alternatives.

Index Terms—Instance-level human parsing, Anchor-free, Edge-guided parsing, Parsing refinement, Video human parsing.

I. INTRODUCTION

INSTANCE-LEVEL human parsing is a fundamental challenge in the fields of computer vision and multimedia, which focuses on pixel-wise human-centric analysis in the world. It aims to not only distinguish various human instances but also segment each instance into accurate human parts. Accordingly, instance-level human parsing can provide human details of each instance, which plays an active role in human-related tasks, such as dense pose estimation [1, 2], person

This work is supported in part by the Shenzhen sustainable development project (No. KCXFZ20201221173013036), in part by National Natural Science Foundation of China (No. 62132006, U2001202), and in part by Open Project Program of State Key Laboratory of Virtual Reality Technology and Systems, Beihang University (No.VRLAB2021C06) (Corresponding author: Xiaochun Cao.)

S. Zhang is with the State Key Laboratory of Information Security, Institute of Information Engineering, Chinese Academy of Sciences, Beijing 100093, China, and also with Georgia Tech Shenzhen Institute, Tianjin University, Shenzhen, 518055, China (e-mail: zhangsanyi@iie.ac.cn).

X. Cao is with School of Cyber Science and Technology, Shenzhen Campus, Sun Yat-sen University, 518107, China (e-mail: caoxiaochun@mail.sysu.edu.cn).

G.-J. Qi is with Futurewei Technologies, Seattle, WA, 98006, USA (e-mail: guojunq@gmail.com).

Z. Song is with Georgia Tech Shenzhen Institute, Tianjin University, Shenzhen, 518055, China (e-mail: zhanjiesong@tju.edu.cn).

J. Zhou is with the Department of Automation, Tsinghua University, Beijing 100084, China (e-mail: jzhou@tsinghua.edu.cn).

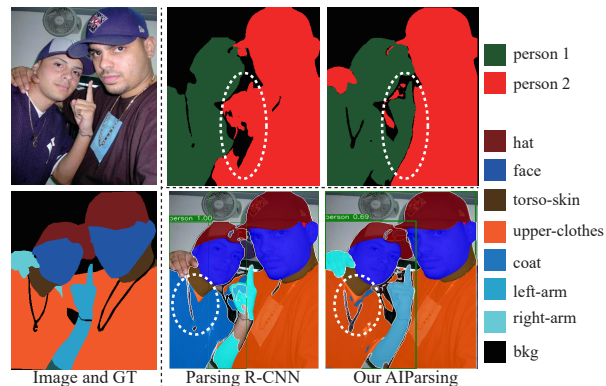


Fig. 1. The motivation of the proposed AIParsing. From the two indicated regions (with white color), our proposed AIParsing can distinguish different instance regions (first row) and boundaries among adjacent human parts (second row) than Parsing R-CNN [2] while equipped with the same ResNet-50 backbone.

re-identification [3, 4], human-object interaction [5–8], visual try-on [9, 10], fashion editing [11], human part analysis [12], fashion landmark detection [13], human-centric video analysis in complex events [14], and so on.

Recently, Mask R-CNN [15] and its improvements [16–19] have made great progress in instance segmentation tasks. Following the same spirit, current state-of-the-arts on instance-level human parsing still follow the Mask R-CNN [15] model. Specifically, the end-to-end framework of the RP R-CNN [20] which utilizes a two-stage human instance detector (*i.e.*, Faster R-CNN [21]) to extract anchor-based region proposals and conduct fine-grained human part parsing.

Inevitably, the current two-stage anchor-based human detector has two limitations. First, the performance of the two-stage object detector is sensitive to hyper-parameters pre-defined in the anchor generation [21, 22], *e.g.*, aspect ratio, anchor area, and scale, *etc.* We need to carefully tune or re-design anchor boxes for new datasets or new detection tasks. Furthermore, choosing suitable bounding box samples with a high recall rate and controlling the imbalance rate of positive and negative samples cause extra computational and memory costs. Second, the two-stage anchor-based detector is not per-pixel prediction oriented, which limits the consistency of the per-pixel parsing module in the human instance parsing task. Thus, exploring a fully convolutional solvable, anchor-free and one-stage detector that avoids hyper-parameter sensitivity meets the need of human instance analysis tasks. To segment human instances with fine-grained categories, the fully convolutional

networks based detector is beneficial to incorporate detection and parsing into a unified framework. Thus, FCOS [23] is introduced to detect various human instances because of its per-pixel comprehensive representation and satisfactory human detection results.

Besides, for the instance-level human parsing task, only focusing on a powerful and elegant FCN-wise human detector is insufficient since obtaining accurate instance parsing regions with fine-grained categories is the ultimate goal. Based on this purpose, the edge information, which provides a useful cue for distinguishing the boundaries of adjacent human parts from a single human instance or different instances, is provided by a simple edge prediction branch in parallel with the human parsing branch. Therefore, the instance detector ideally provides accurate bounding box results (see Fig. 1 second row, our method provides relatively correct regions for the right human instance), and the human instance parsing module can focus on the fine-grained classification. As shown in Fig. 1, incorporating edge clues predicts accurate instance regions even though instances are in occlusion, and it is also successful at separating the adjacent human part regions.

What’s more, since instance-level human parsing task not only tackles instance-level detection but also handles part-level parsing, it is near impossible to obtain ideal human parsing results merely using pixel-level cross-entropy loss for optimization. Incorporating instance-level and part-level information provides complementary aspects to enhance the parsing results. For the instance-level aspect, the box-level score, which aims at choosing high-quality predicted bounding boxes through sorting box scores, is useful for improving the instance-level metric scores by filtering out low-quality predicted bounding boxes. For the part-level aspect, since part-level parsing quality is also important where AP^p or IoU metrics care, exploring the structure-aware or part-aware criteria, *e.g.*, IoU loss, is useful to refine the parsing results. With these considerations, a refinement head fusing these two conducive clues is constructed to improve the human parsing results with higher global-level and part-level metric scores.

Consequently, a novel one-stage Anchor-free Instance-level human **Parsing** network (**AIParsing**) is proposed, the network embodies an anchor-free human detector (FCOS) and a novel edge-guided parsing branch to generate instance-level human parsing results. Additionally, a comprehensive metric loss function is employed that covering hierarchical enforcements from pixel-level to instance-level. The proposed AIParsing achieves state-of-the-art global metric score (mIoU) and instance-level metric scores (AP_{vol}^p , AP_{50}^p and PCP_{50}) on two image multiple human parsing datasets, *i.e.*, CIHP [24] and LV-MHP-v2.0 [25]. In addition, the proposed AIParsing also achieves the state-of-the-art performance of 52.2% (AP_{vol}^v) on video instance-level human parsing dataset, *i.e.*, VIP [26]. The main contributions are summarized as follows:

- A FCN-like anchor-free detector is employed to improve the current RPN-based detector, which leads to a FCN-solvable framework fitting the ultimate pixel-wise instance-level parsing task.
- An edge-guided parsing module is proposed to accurately parse human regions, which exploits edge clues

to distinguish the boundaries of adjacent human parts within the instance and overlapping instance regions. Two complementary clues, *i.e.*, mIoU-score and mIoU-loss, are fused to further improve the quality of the parsing results through the box-level score and part-level parsing quality, respectively.

- The proposed AIParsing achieves state-of-the-art parsing results on two popular multi-human parsing image benchmarks (*i.e.*, CIHP [24] and LV-MHP-v2.0 [25]) and one video instance-level human parsing benchmark (*i.e.*, VIP [26]). The proposed AIParsing can also be served as a baseline towards solving instance-level parsing tasks due to the per-pixel nature.

The remaining parts of our paper are as follows. In section II, we introduce the related work. Then, the details of the methodology are presented in Section III. Experiments on two instance-level human parsing image benchmarks and one multi-human parsing video benchmark are discussed in Section IV. Finally, we conclude in Section V.

II. RELATED WORK

In this section, we firstly introduce current anchor-free and anchor-based object detectors, then we will discuss instance-level human parsing related solutions.

A. Anchor-based vs. Anchor-free Object Detector

In the object detection task, there are two mainstream detectors according to the bounding box selection, anchor-based and anchor-free detectors. Generally, anchor-based object detectors generates a series of candidate proposals according to pre-defined anchor sizes first and then performs object classification and bounding-box offset regression on these proposals. Recently, Region Proposal Network (RPN) based anchors have been certificated their high accuracy and effectiveness on the object detection task, such as Faster R-CNN [21], SSD [27], YOLOv2 [28], and YOLOv3 [29]. However, the complex hyper-parameters of anchor-based proposals restrict the generalization capability, we need to carefully design and tune the hyper-parameters for new detection tasks. Moreover, the sampling of anchor boxes also requires complicated computation, such as calculating the Intersection over Union (IoU) with ground-truth boxes. Although these anchor-based methods provide powerful detection accuracy, exploring anchor-free or proposal-free object detectors without heuristic tuning will enhance the generalization ability. Besides, as with other dense prediction tasks, solving object detection in the way of per-pixel prediction will make these vision tasks formulate in a unified framework. Thus, anchor-free or proposal-free detectors are proposed to solve these two problems, which utilize points to predict bounding boxes and make full use of fully convolutional networks, such as DenseBox [30], YOLOv1 [31], CornetNet [32], FCOS [23], ExtremeNet [33], and CenterNet [34]. YOLOv1 [31] predicts bounding boxes at points near the center of objects. CornerNet [32] detects a pair of corners (top-left and bottom-right) of a bounding box and groups them to form the final detected bounding box. In particular, FCOS [23] is an anchor-free per-pixel detection method,

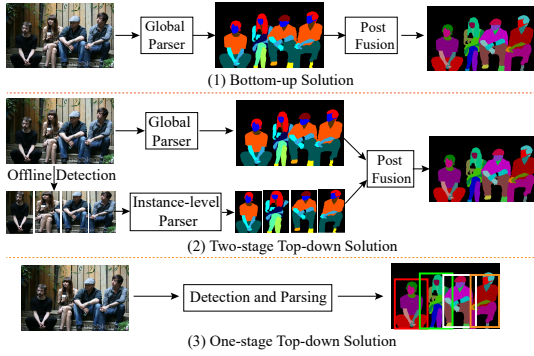


Fig. 2. Different instance-level human parsing solutions.

which predicts a 4-D vector and a class label to represent a bounding box. The 4-D vector is the distance from the location to the four sides of the bounding box. And Anchor-free based detectors are also explored in instance segmentation tasks, like [16, 35–37]. The video instance segmentation task [38, 39] is also inspired by the anchor-free detection for predicting accurate detection and segmentation of the target frame.

B. Instance-level Human Parsing

Current solutions for instance-level human parsing can be divided into three types: bottom-up, two-stage top-down, and one-stage top-down.

Bottom-up: Bottom-up related solutions [24, 40, 41] view the instance-level human parsing task as a global fine-grained semantic segmentation task. They mainly focus on firstly predicting accurate human parsing results on a pixel-level (global parser), and then grouping pixels into different instances according to pre-designed cues (post fusion), as shown in Fig. 2 (1). Gong *et al.* [24] proposes a detection-free bottom-up based Part Grouping Network (PGN) for multi-human parsing. PGN generates human instance results by utilizing extra edge information. Moreover, Graphonomy [41] and Gray-ML [40] explore the underlying label semantic relations in a hierarchical graph structure. These methods can achieve satisfactory results on global human parsing, but the instance-level performance is relatively weak since it lacks the human detection branch. Recently, Zhou *et al.* [42] proposes a novel bottom-up regime (MG-Parsing) that fuses category-level human parsing and multiple human pose estimation into an end-to-end differentiable way. Specifically, a dense-to-sparse projection field connects the dense human parsing annotation with the sparse keypoints, which creates a multi-granularity human representation learning for the instance-level human parsing task.

Two-stage top-down: Unlike bottom-up based methods, two-stage top-down based methods [43–46] firstly adopt a well-trained object detector [47] to detect human instances, then the detected instances are utilized to obtain human instance parsing results, as shown in Fig. 2 (2). Ruan *et al.* [43] proposes a Context Embedding with Edge Perceiving (CE2P) framework for the single human parsing task. Ruan *et al.* [43] also extends CE2P to M-CE2P to deal with the multiple human parsing problem. Specifically, two single human

parsing models trained with detected and ground-truth human instances and one global human parsing model are fused to achieve the final instance-level human parsing results. Liu *et al.* [44] proposes a braiding network which is consisted of two sub-networks, a semantic knowledge learning network and a local structure capturing network. Zhang *et al.* [46] proposes a novel pyramidal gather-excite context network for the single human parsing task and extends it to multiple human parsing. Ji *et al.* [45] proposes to formulate the multiple human part regions into a semantic tree architecture, and a semantic aggregation module is also proposed to combine multiple hierarchical features and exploit the rich context information. Li *et al.* [48] proposes a model-agnostic self-correction mechanism for the human parsing task, which progressively refines labels in an online manner removing the influence coming from label noise. The two-stage top-down methods are mainly devoted to training a robust model for single human parsing. Then human detection mainly relies on the extra Mask R-CNN [15] detector.

One-stage top-down: The difference between two-stage top-down and one-stage top-down lies in that whether the human instance detection and segmentation are designed in an end-to-end manner (as shown in Fig. 2 (3)) or not. Although the two-stage top-down based models usually achieve powerful performance on instance-level human parsing, the inference speed and flexibility is limited if it is deployed on practical systems. Thus, exploring one-stage top-down models is of practical significance. Qin *et al.* [49] proposes a top-down unified framework which simultaneously detects human instances and parse human parts within each instance with an attention module. Zhao *et al.* [25] proposes a top-down Nested Adversarial Network (NAN) for instance-level human parsing, which contains three GAN-like [50] sub-nets, foreground prediction, instance-agnostic parsing, and instance-aware clustering. Yang *et al.* [2] proposes an one-stage top-down model named Parsing R-CNN for instance-level human analysis, which employs anchor-based approaches for human detection and a geometric and context encoding module for human instance parsing. Parsing R-CNN significantly improves the performance of the instance-level parsing metrics. Yang *et al.* [20] also extends Parsing R-CNN to a new RP R-CNN through introducing a global semantic network to enhance the parsing ability and a parsing re-scoring network to get high-quality parsing maps. Our work follows the one-stage top-down design and explores a powerful anchor-free instance-level human parsing framework.

III. METHODOLOGY

The overall pipeline of the Anchor-free Instance-level human Parsing network (**AIParsing**) is shown in Fig. 3. AIParsing contains three main parts: a Feature Pyramid Network (FPN), a human instance detection head, and an edge-guided human instance parsing head. Given an input image, multi-level features are firstly extracted through the FPN-based backbone. Specifically, five levels of feature maps {P3, P4, P5, P6, P7} are used and they own five different strides 8, 16, 32, 64, and 128, respectively. P3, P4, and P5 are generated by

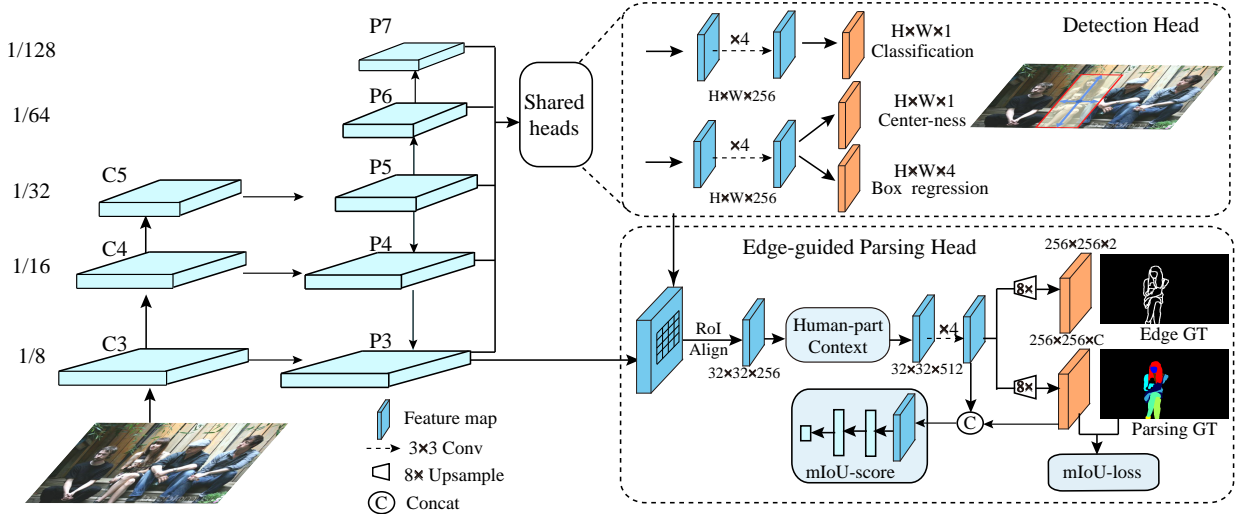


Fig. 3. The overview of our proposed AIParsing framework. Given an input image, a feature pyramid network is firstly used along with a backbone CNN to extract multi-level feature maps. Then the multi-level features are fed to predict human instance bounding boxes through the detection head. And human instance parsing and edge maps are predicted via the edge-guided parsing head.

the CNNs’ feature maps C3, C4, and C5 followed by a 1×1 convolutional layer with the top-down connections [51]. P6 and P7 are produced via a convolutional layer with stride being 2 on P5 and P6, respectively. Then the multi-level features are used to predict human bounding boxes and parsing maps through the detection head and the edge-guided parsing head, respectively.

A. Detection Head

The goal of the detection head is to locate multiple human instances in the input image. In order to obtain accurate human instance bounding boxes, almost all existing instance-level human parsers, such as M-CE2P [43], SemaTree [45], PGECNet [46], Parsing R-CNN [2], choose anchor-based object detectors for human detection, *i.e.*, Faster R-CNN [21], which firstly generate a serial of proposals according to the pre-defined anchor boxes, then execute classification and offset regression. However, the pre-defined anchor boxes need tricky hyper-parameter tuning, which hampers the generality of new datasets or tasks. Moreover, the lack of detail in predictions on a pixel level of two-stage anchor-based detectors does not harmonize with the following dense-pixel parsing task. At present, the Fully Convolutional Networks (FCNs) [52] lead the mainstream frameworks in pixel-wise dense prediction tasks, such as semantic segmentation [52] and scene parsing [53]. For the instance-level human parsing task, the ultimate goal is to segment human instances with fine-grained categories. Therefore, utilizing FCN-based architecture will be more effective since it enables incorporation of the instance detection and parsing tasks into a unified framework. Motivated by FCOS [23], we introduce an anchor-free detector with fully convolutional operations as our human instance detector, which avoids parameter sensitivity related to anchor boxes. As shown in Fig. 3, the detection head is shared from P3 to P7, each position (x, y) of the feature map P_i predicts three outputs: a 4D box offset vector \mathbf{t}^* , a

human classification score and a center-ness score. The 4D bounding box regression vector $\mathbf{t}^* = (l^*, t^*, r^*, b^*)$ denotes the offset distances from the location (x, y) to the left, top, right, bottom sides of the bounding box, respectively. The location (x, y) is corresponding to the bounding box $B_i = (x_0^{(i)}, y_0^{(i)}, x_1^{(i)}, y_1^{(i)}) \in \mathbb{R}^4$, where $(x_0^{(i)}, y_0^{(i)})$ and $(x_1^{(i)}, y_1^{(i)})$ denote the left-top and right-bottom points of the bounding box, and the 4D offset vector \mathbf{t}^* is formulated as:

$$\begin{aligned} l^* &= x - x_0^{(i)}, t^* = y - y_0^{(i)}, \\ r^* &= x_1^{(i)} - x, b^* = y_1^{(i)} - y. \end{aligned} \quad (1)$$

The loss of the detection head is:

$$L_{det} = L_{cls} + L_{reg} + L_{center}, \quad (2)$$

where L_{cls} is the focal loss [22], L_{reg} is the bounding box IoU loss [54] and L_{center} is the binary cross entropy loss. L_{cls} , L_{reg} and L_{center} are the loss of classification, offset regression and center-ness outputs, respectively. The detection head extracts multiple human bounding boxes in the per-pixel prediction manner and feeds them into the following edge-guided parsing branch.

B. Edge-guided Parsing Head

The edge-guided human instance parsing head contains four main parts, *i.e.*, detail-preserving, human-part context encoding, prediction head, and refinement head.

Detail-preserving: As shown in Fig. 3, detail-preserving is performed on P3 via the RoIAlign operation, where P3 is the finest-resolution output feature map of the FPN. There are two reasons for adopting this mechanism according to the character of the instance-level human parsing task. One reason is that we need enough annotated human instances with large sizes to train a robust model since small-size human instances have less appearance information. According to the statistics

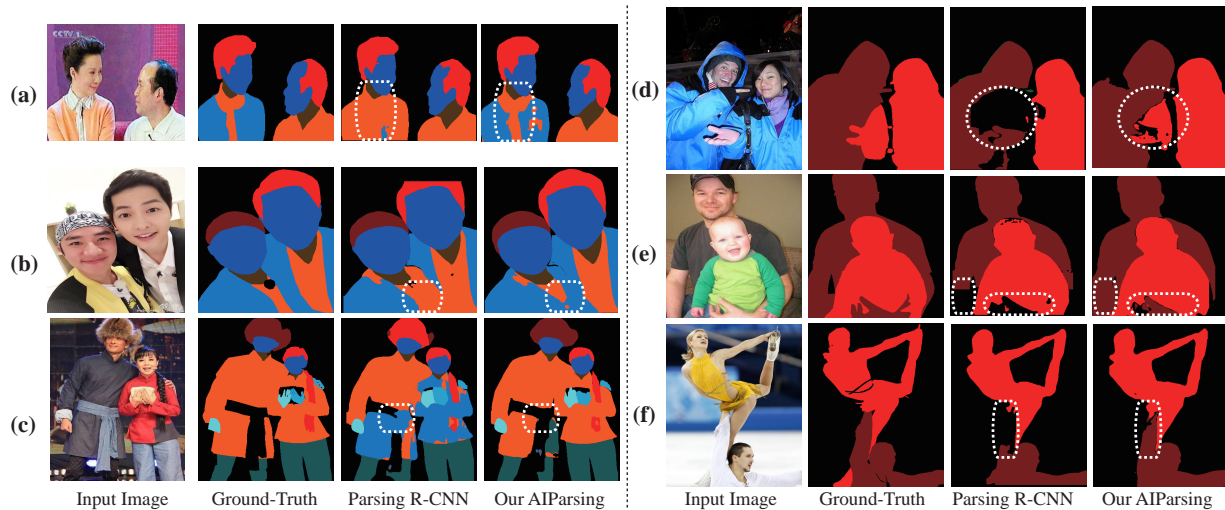


Fig. 4. Illustration of the effectiveness of the edge clue. The first and second columns are the human instance masks and human parsing results, respectively. Both Parsing R-CNN [2] and AIParsing use the same ResNet-50 backbone. Note that the AIParsing is employed without the refinement head for a fair comparison.

in the literature [2], 74% and 86% of human instances in CIHP [24] and LV-MHP v2.0 [25] datasets take up more than 10% area of the image, respectively. The other reason is that coarser-resolution feature maps provide limited appearance representation, especially for small human parts within the instance. If we perform ROI pooling on the coarser resolution (e.g., P7), some small human parts (for example, glove, left-hand, or glass) may be ignored in the coarse layers because of the down-sampling operations. Therefore, finer resolutions are more suitable for this task, as they can provide more detailed appearance information and better segmentation of human instances. Motivated by the high-resolution maintenance strategy used in DeepLabv3+ [55], which utilizes details from low-level feature maps (e.g., conv2) to recover detailed information, here we chose the finest-resolution P3 to perform ROI pooling. It seems insufficient that only performing ROI pooling on P3 may ignore the high-level semantic information. But in fact, the P3 feature map has fused the higher semantic information (C4 and C5) via the FPN, as shown in Fig. 3.

Similar to the feature map selection, the output size of ROI is also important. Generally, the ROI pooling operation in Mask R-CNN [15] projects an ROI region into a feature map with a fixed size of 7×7 (or 14×14). Since we need many details to densely parse the human instance, the desired output size of ROI should also preserve more instance details as possible. However, larger ROI resolution will lead to more computational cost, we chose 32×32 ROI output size as a trade-off in this paper.

Human-part context encoding: The human-part context encoding module is implemented on the outputs of the detail-preserving step. The context information is an important clue in semantic segmentation [55–57] and human parsing tasks [2, 43, 46, 58, 59]. There are two ways to explore the contextual information, *i.e.*, the scale and multi-part relationship. The scale factor is focused on the multi-scale problem. Human parts usually own various scales, hence an effective way to

capture global and local information can help the following human parsing step. Indeed, the feature pyramid is a popular structure that can incorporate multiple scales. Specifically, the Pyramidical Gather-Excite Context module (PGEC) [46] is adopted to detect multi-scale context. Besides, the multi-part relationship provides valuable and relative information between various parts of the person. The context of spatial position typically refers to a series of positions, and the label of a spatial position (pixel) in an image denotes the category of the human part. As a result, constructing a relationship between a spatial position and its context can reflect the relationship between different human parts. Motivated by the self-attention mechanism which can capture long-range dependencies upon spatial positions, non-local operations [60] are employed to explore the relationships between spatial positions.

At last, two types of context information are combined to formulate the human-part context encoding module, which provides rich context representation and helps to identify human parts. Specifically, PGEC contains one 3×3 convolution and four gather-excite units with spatial extent ratios $e = \{4, 8, 16, H\}$. A different point with the original PGEC is that we use five serial depth-wise convolution layers instead of the original one depth-wise convolution layer in GE_H. The non-local operation chooses the embedded Gaussian version with group normalization [61] in the last.

Prediction head: The prediction head contains two tasks, parsing and edge predictions. One motivation for introducing extra edge prediction is to distinguish different human parts from each other in a single human instance. In general, there are various human parts within the human body region, and accurately distinguishing adjacent human parts can assist with segmenting human parts well. As shown in the left column of Fig. 4, AIParsing can predict more accurate regions with the assistance of edge information than Parsing R-CNN. For example, in Fig. 4 (a), two adjacent human parts (*i.e.*, upper clothes and coat in the denoted white box) are hard

to distinguish and while the Parsing R-CNN fails, AIParsing is able to predict accurate parsing results with the help of edge clue. Similar results can be observed from Fig. 4 (b) and (c). Another motivation is that there are various human instances in a detected bounding box, thus it is important to discriminate boundaries between overlapping instances. The edge information has been certificated in single human parsing [43, 46] and semantic segmentation [62, 63], which is an useful clue to distinguish various human parts. The edge clue is also explored on instance segmentation tasks, for example, BMask R-CNN [19] learns object boundaries and masks in an end-to-end manner, which can predict precise boundaries of masks. We extend it to help differentiate different human instances for locating accurate instance regions. Some examples can be referred to the right column of Fig. 4, our AIParsing predicts more precise instance regions compared to Parsing R-CNN. If two human instances share approximate appearances (Fig. 4 (d)), or overlapping regions (Fig. 4 (e)), or adjacent obscure boundaries (Fig. 4 (f)), the proposed AIParsing can provide us with relatively complete regions. The prediction head is implemented on the enhanced context representation. Specifically, a series of four shared convolution layers are conducted, and then two prediction branches, parsing and edge, are followed. The loss of the prediction head is:

$$L_{pred} = \alpha L_{parsing} + \beta L_{edge}, \quad (3)$$

where $\alpha = \beta = 2$. $L_{parsing}$ is the standard cross-entropy loss. L_{edge} is the weighted cross-entropy loss, the formulation is:

$$L_{edge} = -w_0 \sum_{i \in Y_-} \log(p_i(y_i = 0)) - w_1 \sum_{i \in Y_+} \log(p_i(y_i = 1)), \quad (4)$$

where $w_0 = \frac{|Y_+|}{|Y|}$, $w_1 = \frac{|Y_-|}{|Y|}$. Y_- and Y_+ are the ground-truth pixels belonging to non-edge and edge, respectively. $p_i(\cdot)$ denotes the probability of i -th pixel.

Refinement head: While the parsing prediction results are obtained through the prediction head, they are still not ideal. There are two main problems upon the predicted bounding boxes, *i.e.*, low-quality global-level box and imprecise part-level parsing map. The low-quality predicted bounding boxes with inaccurate regions will lead to lower IoU scores, and influence the instance-level AP scores. Meanwhile, if the parsing maps are with imprecise predictions, they will cause lower IoU scores on some human classes, and will result in an unsatisfactory global-level parsing mIoU score. Thus, these two issues should be fused in a complementary manner, where the global-level box focuses on improving the quality of the predicted bounding boxes, and the part-level parsing maps focus on improving the quality of each human class. Specifically, the global-level boxes are optimized through a re-scoring subnetwork estimating the mIoU score of the predicted human instance parsing map within the detected bounding box, where the subnetwork consists of two convolution layers and three fully connected layers. The part-level parsing results are implemented via optimizing a structure-aware tractable surrogate loss (mIoU loss) [67]. The loss of the refinement head is:

$$L_{refine} = \theta L_{miou} + \gamma L_{miou-score}, \quad (5)$$

where L_{miou} is the parsing mIoU loss [67], and $L_{miou-score}$ adopts the MSE loss, $\gamma = 1, \theta = 2$.

The total loss of AIParsing L_{total} is the sum of the detection head L_{det} , the prediction head L_{pred} , and the refinement head L_{refine} .

IV. EXPERIMENTS

In this section, we evaluate the proposed Anchor-free Instance-level human Parsing network (AIParsing) on two popular image instance-level human parsing datasets, *i.e.*, CIHP [24] and LV-MHP-v2.0 [25], and one video multiple human parsing benchmark, *i.e.*, VIP [26].

A. Datasets and Metrics

CIHP: Crowd Instance-level Human Parsing (CIHP) [24] is a large-scale multiple human parsing dataset in the wild. There are 38,280 human images in total, which are annotated with 19 pixel-wise human semantic parts and instance-level human IDs. The whole dataset is split into three parts: 28,280 images for training, 5,000 images for validation, and 5,000 images for testing, respectively.

LV-MHP-v2.0: Learning Vision Multi-Human Parsing (LV-MHP-v2.0) [25] is also a large-scale challenge instance-level human parsing dataset captured in real-world scenes from various conditions. LV-MHP-v2.0 contains 25,403 images, each image is annotated with 58 fine-grained semantic category labels and contains 2-26 persons. 15,403, 5000, 5000 images are used for training, validation, and testing, respectively.

VIP: Video Instance-level Parsing (VIP) [26] dataset is a large-scale video-based multiple human parsing benchmark. There are 404 videos in total and 20 annotated semantic part labels (same with CIHP). VIP is divided into three parts, 304 videos for training, 50 videos for validation, and 50 videos for testing, respectively. The frames in the training and validation set are 16,024, and 2,445, respectively.

Metrics: Two types of metrics are evaluated, *i.e.*, global-level and instance-level metrics. For the global parsing metric, the standard mean Intersection over Union (mIoU) score is reported. For local-sensitive instance-level evaluation, the Average Precision based on part (AP^p) is adopted to evaluate the instance-level human parsing performance. Specifically, AP_{vol}^p and AP_{50}^p scores are reported, where AP_{50}^p denotes the IoU threshold equal to 0.5 and AP_{vol}^p is the mean of various IoU thresholds ($IoU \in [0.1, 0.9]$, with 0.1 increment). In addition, the Percentage of Correctly parsed semantic Parts (PCP) metric is used to evaluate the quality within the human instance. The PCP of one human instance is the ratio between the correctly parsed human semantic part number and the total human semantic part number of that human. Specifically, PCP_{50} score is reported. While for video human parsing task, we also adopt another instance-level metric, *i.e.*, average precision based on region (AP^r), which is used to evaluate the performance from the view of each class.

Implementation details: We follow almost all the hyper-parameters in FCOS [23] except for replacing positive score

TABLE I
PERFORMANCE COMPARISON IN TERMS OF mIoU, AP_{vol}^p , AP_{50}^p AND PCP_{50} WITH STATE-OF-THE-ART METHODS ON THE VALIDATION SET OF CIHP [24]. * DENOTES USING COCO PRE-TRAINING [64]. † DENOTES TEST-TIME AUGMENTATION.

Method	Backbone	Epoch	mIoU	AP_{vol}^p	AP_{50}^p	PCP_{50}
Bottom-up:						
PGN† [24]	ResNet-101	80	57.3	35.1	37.5	-
DeepLab v3+† [55]	Xception	100	58.9	-	-	-
Graphonomy† [41]	Xception	100	58.6	-	-	-
CorrPM [65]	ResNet-101	150	60.2	-	-	-
GPM† [40]	Xception	100	60.3	-	-	-
Gray_ML† [40]	Xception	200	60.6	-	-	-
PCNet [66]	ResNet-101	120	61.1	-	-	-
Two-stage top-down:						
BraidNet [43]	ResNet-101	150	60.6	-	-	-
SemaTree [45]	ResNet-101	200	60.9	-	-	-
M-CE2P [43]	ResNet-101	150	63.6	48.9	54.7	-
PGECNet [46]	ResNet-101	150	64.6	-	-	-
SCHP† [48]	ResNet-101	150	67.5	52.0	58.9	-
One-stage top-down:						
Unified [49]	ResNet-101	37	55.2	48.0	51.0	-
Parsing R-CNN [2]	ResNet-50	75	56.3	53.9	63.7	60.1
Mask Scoring [18]	ResNet-50	75	56.0	56.8	68.9	59.9
BMask R-CNN [19]	ResNet-50	75	56.4	54.3	64.6	61.8
Parsing R-CNN* [2]	ResNet-50	75	57.5	54.6	65.4	62.6
RP RCNN [20]	ResNet-50	75	58.2	58.3	71.6	62.2
AIParsing	ResNet-50	75	59.7	59.2	73.1	66.3
Parsing R-CNN* [2]	ResNeXt-101	75	59.8	55.9	69.1	66.2
AIParsing	ResNet-101	75	60.7	60.3	75.2	68.5
AIParsing	ResNeXt-101	75	60.8	60.5	76.0	69.2
Parsing R-CNN*† [2]	ResNeXt-101	75	61.1	56.5	71.2	67.7
RP RCNN† [20]	ResNet-50	150	61.8	61.2	77.2	70.5
AIParsing †	ResNet-50	75	62.5	62.2	78.3	71.6
AIParsing †	ResNet-101	75	63.0	63.1	79.2	71.7
AIParsing †	ResNeXt-101	75	63.3	63.4	79.9	72.3

threshold value 0.03 with 0.05 as suggested in [16]. FPN levels P3 to P7 are with 256 channels. RoIAlign is selected as the RoI pooling operation. In the training stage, the input image scales are randomly sampled from [640, 800] pixels. Then the images are resized to 800 pixels on the short side and 1,333 pixels or less on the long side [16, 23]. AIParsing is trained with Stochastic Gradient Descent (SGD) for about 75 epochs with a mini-batch of 8 images and an initial learning rate of 0.005 then is decreased by a factor of 10 at 50 and 65 epochs, respectively. The weight decay and momentum are set as 0.0001 and 0.9, respectively. We initialize the backbone models with ImageNet pre-trained weights [68]. In the inference stage, the human detection head with FCOS generates 50 high-score human instance boxes, and these boxes are fed into the edge-guided parsing head to predict parsing maps on each RoI. When we inference with test-time augmentation, the shorter side is resized at multiple scales and keep the aspect ratio, and the horizontal flipping is also applied. For CIHP and VIP, we use multiple scales of (500, 600, 700, 800, 850). For LV-MHP-v2.0, the scales are (500, 600, 700, 800, 850, 1000).

B. Comparison with State-of-the-art Methods

To validate the effectiveness of AIParsing, we analyzed the comparison results with state-of-the-art bottom-up, one-stage, and two-stage top-down parsing methods on CIHP [24] and

LV-MHP-v2.0 [25] validation sets, respectively. In addition, we also certificate our proposed AIParsing on the video human parsing dataset, *i.e.*, VIP [26].

CIHP: We analyzed the comparison results from two views, the global-level metric (mIoU) and the instance-level metrics (AP_{vol}^p , AP_{50}^p and PCP_{50}).

1) **For the global parsing metric**, as shown in Table I, the proposed AIParsing outperforms all one-stage top-down methods in terms of mIoU score. While using the same backbone ResNet-50, the proposed AIParsing achieves 1.5% performance improvement compared to RP R-CNN [20] in terms of mIoU score. Parsing R-CNN adopts MS-COCO [64] pre-training to enhance the parsing ability, conversely, our proposed AIParsing without COCO pre-training can obtain better performance with ResNeXt-101-32x8d backbone (60.8% vs. 59.8%) comparing with Parsing R-CNN. While using test-time augmentation, AIParsing achieves the best mIoU score of 63.3% over all one-stage top-down ones. We can find that the mIoU score of AIParsing is inferior to the best two-stage top-down method SCHP [48]. The best mIoU performance shows that the two-stage top-down methods are good at obtaining global parsing results. It benefits from the two-stage top-down method that improves the global parsing performance through training three independent parsing models, *i.e.*, one global parsing model and two instance-level parsing models. The final global parsing results are acquired by fusing these three parsing models in the inference step. However, two-

TABLE II
PERFORMANCE COMPARISON IN TERMS OF mIoU, AP_{vol}^p , AP_{50}^p AND PCP_{50} WITH STATE-OF-THE-ART METHODS ON THE VALIDATION SET OF LV-MHP-v2.0 [25]. * DENOTES USING COCO PRE-TRAINING [64]. † DENOTES TEST-TIME AUGMENTATION.

Method	Backbone	Epoch	mIoU	AP_{vol}^p	AP_{50}^p	PCP_{50}
Bottom-up:						
MH-Parser [69]	ResNet-101	-	-	36.1	18.0	27.0
NAN [25]	-	80	-	41.7	25.1	32.2
MG-Parsing [42]	ResNet-101	150	41.4	44.3	39.0	42.3
Two-stage top-down:						
SemaTree [45]	ResNet-101	200	-	42.5	34.4	43.5
M-CE2P [43]	ResNet-101	150	41.1	42.7	34.5	43.8
SCHP† [48]	ResNet-101	150	45.2	45.3	35.1	48.0
One-stage top-down:						
Mask R-CNN [15]	ResNet-50	-	-	33.8	14.9	25.1
Parsing R-CNN [2]	ResNet-50	75	36.2	39.5	24.5	37.2
Parsing R-CNN* [2]	ResNet-50	75	37.0	40.3	26.6	40.0
RP RCNN [20]	ResNet-50	75	37.3	45.2	40.5	39.2
AIParsing	ResNet-50	75	39.9	45.9	41.1	45.3
Parsing R-CNN* [2]	ResNeXt-101	75	40.3	41.8	30.2	44.2
Parsing R-CNN*† [2]	ResNeXt-101	75	41.8	42.7	32.5	47.9
AIParsing	ResNet-101	75	40.1	46.6	43.2	47.3
AIParsing	ResNeXt-101	75	40.4	47.5	45.0	48.7
AIParsing †	ResNet-101	75	42.1	49.3	51.3	54.9
AIParsing †	ResNeXt-101	75	42.4	49.9	52.8	56.1

TABLE III
PERFORMANCE COMPARISON WITH STATE-OF-THE-ART METHODS ON THE VALIDATION SET OF VIP [26]. * DENOTES DIRECTLY TESTED ON THE WELL-TRAINED AIPARSING MODEL WITH CIHP DATASET.

Method	mIoU	AP_{50}^r	AP_{60}^r	AP_{70}^r	AP_{80}^r	AP_{90}^r	AP_{vol}^r	AP_{vol}^p	AP_{50}^p	PCP_{50}
DFF [70]	35.3	20.3	15.0	9.8	-	-	20.3	-	-	-
FGFA [71]	37.5	24.0	17.8	12.2	-	-	23.0	-	-	-
ATEN [26]	37.9	25.1	18.9	12.8	-	-	24.1	-	-	-
SCHP [48]	63.2	57.8	52.9	46.3	34.1	12.4	51.4	-	-	-
AIParsing *	60.4	58.9	53.9	45.9	31.6	10.5	51.5	63.8	80.7	70.2
AIParsing	61.4	59.3	54.2	47.7	34.5	12.6	52.2	64.2	81.6	71.1

stage top-down methods are not end-to-end, which limits the practicability in the real-world scene. Bottom-up and one-stage top-down methods are end-to-end, which are encouraged for practical applications. The state-of-the-art one-stage top-down method RP R-CNN [20] and our AIParsing both attain better mIoU scores than all bottom-up methods. Consequently, the proposed AIParsing is effective in obtaining better global parsing performance, it also owns higher instance-level metric scores. However, the two-stage top-down methods fall drastically on instance-level metrics, we will analyze the reasons in the following.

2) **For the instance-level parsing metrics**, as shown in Table I, RP R-CNN [20] with ResNet-50 backbone achieves 6.3% and 12.7% gains than SCHP [48] with ResNet-101 backbone in terms of AP_{vol}^p and AP_{50}^p , respectively. The reason lies in that human detection and parsing steps of two-stage top-down methods are separated, and the detector depends on extra well-trained object detectors without further training. Thus, these two steps trained in parallel in one-stage top-down methods will obtain better instance-level metric scores. With the same ResNet-50 backbone, AIParsing obtains state-of-the-art results and outperforms the runner-up RP R-CNN [20] by large margins of 0.9% AP_{vol}^p / 1.5% AP_{50}^p / 4.1% PCP_{50} . These large margins benefit from the effectiveness of the anchor-free motivation and the useful design of the edge-

guided human instance parsing branch. The large superiority still exists on test-time augmentation results. While using a deeper ResNeXt-101-32x8d backbone, AIParsing attains total suppression compared to Parsing R-CNN in terms of all instance-level parsing metrics. The proposed AIParsing with single-scale testing even outperforms Parsing R-CNN with multi-scale testing both on AP_{vol}^p and PCP_{50} . Further, AIParsing with multi-scale testing obtains the best instance-level parsing metric scores upon all state-of-the-art methods and the satisfactory global-level mIoU score.

LV-MHP-v2.0: We also report the evaluation metric scores of the AIParsing on the LV-MHP-v2.0 validation set, as shown in Table II. The proposed AIParsing equipped with ResNet-50 backbone can achieve better performance than RP R-CNN [20] and Parsing R-CNN [2] on both global-level and instance-level metrics. Specifically, AIParsing outperforms 2.6% mIoU than RP R-CNN [20] with the same ResNet-50 backbone. When a deeper ResNeXt-101-32x8d backbone with test-time augmentation is adopted, AIParsing also obtains the best performance with 42.4% / mIoU, 49.9% / AP_{vol}^p , and 56.1% / PCP_{50} .

VIP: Except image instance-level human parsing data, we further report the comparison metric scores of AIParsing on the video human parsing data, *i.e.*, VIP validation set, as shown in Table III. Because CIHP and VIP share the same human parts,

TABLE IV
ANCHOR-BASED VS. ANCHOR-FREE DETECTORS COMPARISON ON THE
VALIDATION SET OF CIHP [24].

Method	mAP ^{bbbox}	mIoU	AP ^p _{vol}	PCP ₅₀
RPN-parsing	65.8	52.8	51.2	55.3
Anchor-free-parsing	71.4	54.0	52.5	59.8

TABLE V
DIFFERENT ROI OUTPUT SIZES COMPARISON ON THE VALIDATION SET OF
CIHP [24]. FLOPS IS ONLY COMPUTED ACCORDING TO THE
MULTI-SCALE CONTEXT MODULE PGEC.

RoI size	FLOPs(G)	mIoU	AP ^p _{vol}	AP ^p ₅₀	PCP ₅₀
14 × 14	1.2	51.4	50.0	54.4	55.0
32 × 32	6.4	54.0	52.6	60.5	59.6
48 × 48	14.5	54.7	53.6	62.9	61.1

thus we test the performance on VIP val directly adopting the pre-trained AIParsing model with CIHP dataset (denoted it as AIParsing*). The performance (AP^r_{vol}) of AIParsing* is close to current state-of-the-art method SCHP, which shows the generalization ability of the AIParsing. Further, we also provide the results of AIParsing trained with VIP training set. AIParsing can obtain the best instance-level metric score, *i.e.*, 52.2% AP^r_{vol}. The observations from VIP are similar to the image datasets where the proposed AIParsing owns superiority on the instance-level metrics.

C. Ablation Study

In this section, we analyze each part’s effectiveness of AIParsing. Unless specified, all ablation studies are conducted on the CIHP validation set using AIParsing with ResNet-50-FPN backbone and trained for 25 epochs.

Anchor-based detector vs. Anchor-free detector: We use the anchor-based human parsing model Parsing R-CNN [2] as our baseline in this setting, and we directly borrow the evaluation score from literature [2], which is trained for 25 epochs, and we denote it as RPN-parsing. For further comparison, we just replaced the RPN in Parsing R-CNN with an anchor-free FCOS detector while other parts are kept the same, and denote it as Anchor-free-parsing. As shown in Table IV, anchor-free-parsing model improves the mAP^{bbbox} score by about 5.6% compared with the RPN-parsing model, thus shows that the one-stage anchor-free human detector FCOS can achieve better performance than the anchor-based detector. When the detection model obtains better performance, this will help to improve the performance of global-level and instance-level parsing metrics, and thus Anchor-free-parsing obtains higher AP^p_{vol} and PCP₅₀ scores than RPN-parsing. Besides, its per-pixel design style is consistent with the following human instance parsing task.

RoI output size: The RoI size is important for dense human instance parsing since parsing needs sufficient human details to distinguish various parts of a human instance. From our common sense, a larger RoI size owns more details than a small one. However, a large RoI size will generate more memory and computational cost. In Table V, three different RoI sizes, *i.e.*, 14 × 14, 32 × 32, and 48 × 48, are employed to

validate. Although the 14 × 14 size holds fewer computations, it obtains lower performance than the 32 × 32 on all metrics. With a larger 48 × 48, it can obtain better scores than the 32 × 32. However, the large size needs more computational cost by observing the FLOPs. Therefore, we choose the RoI size 32 × 32 as a trade-off.

Human-part context: Human-part context is an effective module in capturing multi-scale context information (PGEC) and the relationship of various human parts (non-local). In Table VI, both the PGEC part and the non-local part have the ability to on improving all metric scores. This shows the effectiveness of each part in the human-part context module. If these two parts are simultaneously added, a 4.4% improvement in terms of mIoU score is achieved. For instance-level metrics, the human-part context module (PGEC+Non-local) obtains 6.8%, 17.4%, 11.7% improvements than the baseline model in terms of AP^p_{vol}, AP^p₅₀ and PCP₅₀, respectively. It shows the effectiveness of exploiting scale and relationship clues to assist in human instance parsing.

Edge information: Introducing edge clues is useful to distinguish adjacent human semantic parts and different instances. The edge label can be obtained by pre-processing the labeled human instance parsing map without extra annotation cost. Specifically, we scan and apply the XOR operation to the neighboring pixels, and use a 3 × 3 kernel implemented on the parsing label to extract the edge pixels. From the performance comparison results in Table VI, the edge information can achieve 0.8% improvement than human-part context based method in terms of mIoU. Meanwhile, instance-level parsing metrics also have 1.2%, 2.2%, 1.9% improvements than human-part context based method in terms of AP^p_{vol}, AP^p₅₀, and PCP₅₀, respectively.

Group normalization: To obtain better performance, group normalization (GN) [61] is introduced to ensure the stability of the training stage. We add the GN operation after the last convolutional layer of the prediction head. Specifically, the method with GN improves 0.8%, 0.6%, 1.7% and 1.3% compared with the ablative method without GN in terms of mIoU, AP^p_{vol}, AP^p₅₀, and PCP₅₀, respectively. The good performance shows the effectiveness of introducing group normalization into the parsing module.

Refinement head: As show in Table VI, if we employ box-level mIoU score to filter out low-quality bounding boxes, it will give more helps on instance-level metric scores, *i.e.*, AP^p_{vol} and AP^p₅₀. The reason lies in that some detected bounding boxes own high confidence scores but low-quality predicting results, these boxes will hurt the mIoU score and further lead to unideal AP^p score. While we combine box-level mIoU score and confidence score to estimate the quality of the detected bounding boxes, these poorly predicted bounding boxes will be discarded. Thus, the AP^p score obtains improvement. However, the optimization of mIoU-score only considers the global-level quality of the detected bounding boxes, but the parsing quality of each part within the detected ones is also important. When we add the part-level constraint, *i.e.*, equipped with mIoU-loss, the method improves 2.0% mIoU score compared with without this constraint. The advantage of the mIoU metric score proves that the high-quality parsing

TABLE VI
DIFFERENT COMPONENTS COMPARISON OF THE EDGE-GUIDED PARSING BRANCH ON THE VALIDATION SET OF CIHP [24].

ResNet50-FPN	Human-part context		Edge	GN	Refinement head		3x	mIoU	AP _{vol} ^P	AP ₅₀ ^P	PCP ₅₀
	PGEC	Non-local			mIoU-loss	mIoU-score					
✓								49.6	45.8	43.1	47.9
✓	✓							52.5	50.8	55.6	56.6
✓		✓						52.7	50.7	55.7	56.0
✓	✓	✓						54.0	52.6	60.5	59.6
✓	✓	✓	✓					54.8	53.8	62.7	61.5
✓	✓	✓	✓	✓				55.6	54.4	64.4	62.8
✓	✓	✓	✓	✓	✓			57.6	54.4	64.8	63.9
✓	✓	✓	✓	✓		✓		55.8	56.8	69.1	62.1
✓	✓	✓	✓	✓	✓	✓		57.3	56.9	69.4	64.4
✓	✓	✓	✓	✓	✓	✓	✓	59.7	59.2	73.1	66.3

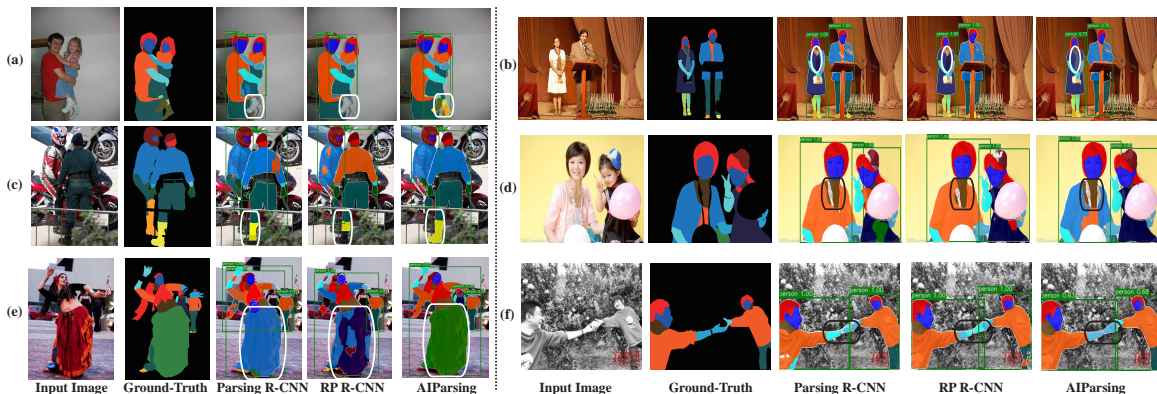


Fig. 5. Visual comparison on CIHP val. AIParsing obtains accurate predictions than Parsing R-CNN [2] and RP R-CNN [20] equipped with same ResNet-50 backbone. The regions labeled in red boxes denote the improved parsing results by our AIParsing.

map assists in obtaining better global parsing results. Here, the AP^P scores are close whether with mIoU-loss constraint or not, the main reason lies in that the selected low-quality detected bounding boxes with high confidence scores lead to approximate scores. When we combine these two useful parts together, it obtains 1.7%, 2.5%, 5.0%, 1.6% improvements than the ablative method without them in terms of mIoU, AP_{vol}^P, AP₅₀^P, and PCP₅₀, respectively. The good performance of the refinement head encourages us to taking these clues into account.

Longer schedule: Increasing iterations or epochs is a useful mechanism to improve performance [2]. As shown in Table VI, we report the performance of adopting three times standard training schedule (25 epochs, denoted as 1×), *i.e.*, 75 epochs in total, denoted as 3×. While training the model with 3× epochs, the mIoU performance is improved by 2.4% compared with that of 1× epoch.

Effectiveness of GN and 3x: For a fair comparison, we chose Parsing R-CNN [2] trained with 3× (75 epochs) and GN as the baselines, while the proposed AIParsing method discards the refinement head, as shown in Table VII. If we replace the Parsing R-CNN with the same FCOS detector, the detection score mAP^{bbbox}, AP and PCP scores can be boosted much more. Moreover, if we add the edge-guided parsing head without containing the refinement part, AIParsing(w/o refine) outperforms Parsing R-CNN in all metric scores.

Different Multi-scale Context: We choose PSP [72] and

TABLE VII
PERFORMANCE COMPARISON ON CIHP VAL. * DENOTES THE RESULTS FROM [20].

Method	mAP ^{bbbox}	mIoU	AP _{vol} ^P	AP ₅₀ ^P	PCP ₅₀
Parsing R-CNN [2]	68.7	56.3	53.9	63.7	60.1
Parsing R-CNN(w/ GN)*	–	56.2	54.2	64.6	60.9
Parsing R-CNN(w/ FCOS)	72.0	56.3	54.5	65.2	63.5
AIParsing(w/o refine)	73.3	57.9	56.1	68.3	66.3

TABLE VIII
DIFFERENT MULTI-SCALE CONTEXT MODULES ON CIHP VALIDATION SET.

Multi-scale Context	mIoU	AP _{vol} ^P	AP ₅₀ ^P	PCP ₅₀
PSP [72]	53.1	52.0	59.1	57.7
ASPP [55]	53.2	52.4	59.8	58.5
PGEC [46]	54.0	52.6	60.5	59.6

ASPP [55] for multi-scale context comparison, as shown in Table VIII. Here we just choose the FPN and human-part context encoding part for comparison. The differences are that we use PSP or ASPP to replace the PGEC module. We can find that the PGEC module is superior than PSP and ASPP modules both on global-level (mIoU) and instance-level (AP_{vol}^P, AP₅₀^P, PCP₅₀) metric scores. The good performance shows that the PGEC module is more suitable than PSP and ASPP for the human parsing task.

Runtime Analysis: We choose the CIHP validation set for runtime analysis, and we compare with three bottom-up based methods (PGN [24], Graphonomy [41], GPM [40]) and two

TABLE IX
INFERENCE TIME COMPARISON ON CIHP VALIDATION SET.

Method	mIoU	Backbone	Params (M)	FPS
PGN [24]	54.4	ResNet-101	629.2	4.2
Graphonomy [41]	55.5	Xception	156.9	25.0
GPM [40]	56.2	Xception	176.0	16.6
Parsing R-CNN [2]	56.3	ResNet-50	54.3	7.4
RP R-CNN [20]	58.2	ResNet-50	58.4	5.0
AIParsing	59.7	ResNet-50	50.2	8.9
AIParsing-light	56.7	ResNet-50	28.5	13.3

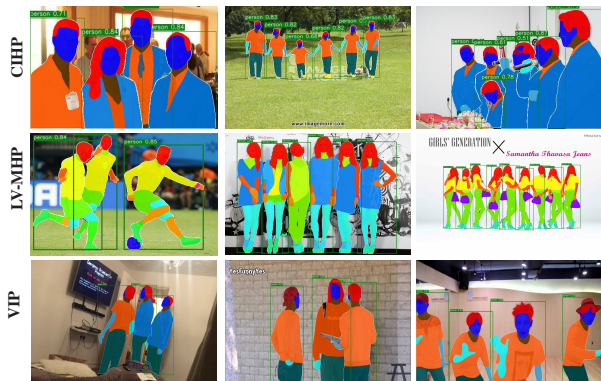


Fig. 6. Visualization results on CIHP [24], LV-MHP-v2.0 [25] and VIP [26] val sets. The boxes with green color denote the human detection results.

one-stage top-down instance-level human parsing methods (Parsing R-CNN [2] and RP R-CNN [20]). For a fair comparison, all methods are conducted on a single NVIDIA GeForce RTX 2080 Ti GPU with 11GB memory, the comparison results are shown in Table IX. The bottom-up based Graphonomy model can obtain the best FPS score compared with other methods. However, the Params of Graphonomy equipped with Xception backbone is larger than the proposed AIParsing-lite with ResNet-50 backbone. Meanwhile, the mIoU score of AIParsing-lite is superior to the Graphonomy method. Our proposed AIParsing can obtain a better mIoU score and inference faster than other one-stage top-down parsing methods. The advantage benefits from the anchor-free FCN-like design. To further explore a faster inference model, we designed a lighter AIParsing model to accelerate, which is named AIParsing-light. Specifically, except for the backbone part, the channels of all conv layers are reduced by half. The number of serial conv layers for predicting branches in the detection head and edge-guided parsing head is also reduced by half. In addition, the input image scales are randomly sampled from [580, 600] pixels, and the images are resized to 600 pixels on the short side and 1,000 pixels or less on the long side. Other settings are the same as the standard AIParsing model. As shown in Table IX, although the parsing performance of AIParsing-light is worse than other methods, the AIParsing-light model owns fewer parameters and faster inference time than other comparison methods where it can run at 13.3 FPS.

D. Qualitative Results

In Fig. 5, we visualize some qualitative comparison results with state-of-the-art one-stage top-down human parsing meth-

ods, all methods employ the same ResNet-50 backbone for fair comparison on CIHP validation set. As shown in Fig. 5, we can see that the proposed AIParsing can obtain better parsing results of adjacent human parts and more accurate instance regions than Parsing R-CNN [2] and RP R-CNN [20]. The human parsing results are usually influenced by the human detection results, if we predict accurate regions of the human instance, better parsing results will be obtained. As shown in Fig. 5 (a), (c), (f), our AIParsing provides relatively complete regions (denoted as quadrilateral regions) than Parsing R-CNN and RP R-CNN, especially in some challenging scenes, such as occlusion or appearance approximation. In Fig. 5 (f), the arm regions of two human instances are hard to distinguish. Benefit from taking the edge information into account, the model can distinguish two instance regions well. In Fig. 5 (b), the proposed AIParsing predicts a more accurate scarf region than other ones (refer to the white elliptic region). The proposed AIParsing predicts high-quality parsing results for the adjacent human part region, as shown in Fig. 5 (b) and (d). These results reveal that our proposed method has the superiority of dealing with cases in the real-world scene.

Besides, we also show more visualization results obtained by our proposed AIParsing. Specifically, the qualitative results of AIParsing with a ResNeXt-101-32x8d backbone are shown in Fig. 6, which are obtained from the validation sets of CIHP [24], LV-MHP-V2.0 [25] and VIP [26], respectively. The experimental results demonstrate the effectiveness of the proposed AIParsing in various scenes, such as crowded scenes, overlapping instances, complex human poses, and so on. More visualization results can be found in the supplementary file.

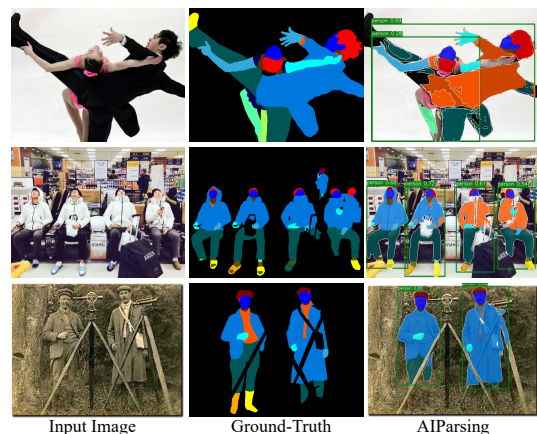


Fig. 7. Some failure cases obtained from CIHP dataset.

Failure Cases: In some cases, the proposed AIParsing fails to obtain ideal parsing results, as shown in Fig. 7, for example, highly overlapped instances, close human classes, and the human instance region is close to the background. For the first row of Fig. 7, these two human instances are highly overlapped, and the parsing result fails to accurately locate the instance region. For the second row of Fig. 7, four human instances are with the same coats, but the parsing results are not consistent in these regions. For the third row of Fig. 7, the background color is similar to the human instances, the anchor-free human detector fails to locate the whole instance

region. Thus, in the future, the multiple human parsers should improve the ability of dealing with highly overlapped instances and similar backgrounds, and consider the relationships among different human instances to avoid the inconsistent result in the same image.

V. CONCLUSION

In this paper, we propose a novel Anchor-free Instance-level human Parsing network (AIParsing), which fuses an anchor-free detector head and an edge-guided parsing head into a unified framework. The anchor-free detector has been certificated that it owns better ability than the anchor-based detector. In addition, edge information also provides help to distinguish adjacent human parts and overlapping instances. A refinement head is employed to enhance the parsing result through box-level mIoU-score and part-level mIoU-loss. The proposed AIParsing outperforms current state-of-the-art methods especially on instance-level parsing metrics on two multiple human parsing datasets (*i.e.*, CIHP and LV-MHP-v2.0) and one video human parsing dataset (*i.e.*, VIP). We hope the FCN-like AIParsing model can be extended to solve other instance-level dense prediction tasks in a more detailed per-pixel fashion. Human structure is an important clue to help to parse the human parts well, which has been well certificated in human parsing tasks [73, 74]. The core idea is to parse the human on multiple levels. Thus, how to design a reasonable network taking the human structure into account needs further discussion in the future. In addition, how to utilize instance-level human parsing technology solving the problems of human-centric video analysis [14] especially in complex events is worth studying.

REFERENCES

- [1] Rıza Alp Güler, Natalia Neverova, and Iasonas Kokkinos. Densepose: Dense human pose estimation in the wild. In *Proc. IEEE Conf. CVPR*, pages 7297–7306, 2018.
- [2] Lu Yang, Qing Song, Zhihui Wang, and Ming Jiang. Parsing r-cnn for instance-level human analysis. In *Proc. IEEE Conf. CVPR*, pages 364–373, 2019.
- [3] Wei Li, Xiatian Zhu, and Shaogang Gong. Harmonious attention network for person re-identification. In *Proc. IEEE Conf. CVPR*, pages 2285–2294, 2018.
- [4] Jiaxu Miao, Yu Wu, Ping Liu, Yuhang Ding, and Yi Yang. Pose-guided feature alignment for occluded person re-identification. In *Proc. IEEE Conf. ICCV*, pages 542–551, 2019.
- [5] Yu-Wei Chao, Zhan Wang, Yugeng He, Jiakuan Wang, and Jia Deng. Hico: A benchmark for recognizing human-object interactions in images. In *Proc. IEEE Conf. ICCV*, pages 1017–1025, 2015.
- [6] Georgia Gkioxari, Ross Girshick, Piotr Dollár, and Kaiming He. Detecting and recognizing human-object interactions. In *Proc. IEEE Conf. CVPR*, pages 8359–8367, 2018.
- [7] Siyuan Qi, Wenguan Wang, Baoxiong Jia, Jianbing Shen, and Song-Chun Zhu. Learning human-object interactions by graph parsing neural networks. In *Proc. ECCV*, pages 401–417, 2018.
- [8] Tianfei Zhou, Siyuan Qi, Wenguan Wang, Jianbing Shen, and Song-Chun Zhu. Cascaded parsing of human-object interaction recognition. *IEEE Transactions on Pattern Analysis and Machine Intelligence (TPAMI)*, 2021.
- [9] Chia-Wei Hsieh, Chieh-Yun Chen, Chien-Lung Chou, Hong-Han Shuai, Jiaying Liu, and Wen-Huang Cheng. Fashionon: Semantic-guided image-based virtual try-on with detailed human and clothing information. In *Proc. ACM MM*, pages 275–283, 2019.
- [10] Haoye Dong, Xiaodan Liang, Xiaohui Shen, Bochao Wang, Hanjiang Lai, Jia Zhu, Zhiting Hu, and Jian Yin. Towards multi-pose guided virtual try-on network. In *Proc. IEEE Conf. ICCV*, pages 9026–9035, 2019.
- [11] Haoye Dong, Xiaodan Liang, Yixuan Zhang, Xujie Zhang, Xiaohui Shen, Zhenyu Xie, Bowen Wu, and Jian Yin. Fashion editing with adversarial parsing learning. In *Proc. IEEE Conf. CVPR*, pages 8120–8128, 2020.
- [12] Lu Yang, Qing Song, Zhihui Wang, Mengjie Hu, and Chun Liu. Hier r-cnn: Instance-level human parts detection and a new benchmark. *IEEE Transactions on Image Processing (TIP)*, 30:39–54, 2021.
- [13] Wenguan Wang, Yuanlu Xu, Jianbing Shen, and Song-Chun Zhu. Attentive fashion grammar network for fashion landmark detection and clothing category classification. In *Proc. IEEE Conf. CVPR*, pages 4271–4280, 2018.
- [14] Weiyao Lin, Huabin Liu, Shizhan Liu, Yuxi Li, Rui Qian, Tao Wang, Ning Xu, Hongkai Xiong, Guo-Jun Qi, and Nicu Sebe. Human in events: A large-scale benchmark for human-centric video analysis in complex events. *arXiv preprint arXiv:2005.04490*, 2020.
- [15] Kaiming He, Georgia Gkioxari, Piotr Dollár, and Ross Girshick. Mask r-cnn. In *Proc. IEEE Conf. ICCV*, pages 2961–2969, 2017.
- [16] Youngwan Lee and Jongyoul Park. Centermask: Real-time anchor-free instance segmentation. In *Proc. IEEE Conf. CVPR*, pages 13906–13915, 2020.
- [17] Kai Chen, Jiangmiao Pang, Jiaqi Wang, Yu Xiong, Xiaoxiao Li, Shuyang Sun, Wansen Feng, Ziwei Liu, Jianping Shi, Wanli Ouyang, et al. Hybrid task cascade for instance segmentation. In *Proc. IEEE Conf. CVPR*, pages 4974–4983, 2019.
- [18] Zhaojin Huang, Lichao Huang, Yongchao Gong, Chang Huang, and Xinggang Wang. Mask scoring r-cnn. In *Proc. IEEE Conf. CVPR*, pages 6409–6418, 2019.
- [19] Tianheng Cheng, Xinggang Wang, Lichao Huang, and Wenyu Liu. Boundary-preserving mask r-cnn. In *Proc. ECCV*, pages 660–676, 2020.
- [20] Lu Yang, Qing Song, Zhihui Wang, Mengjie Hu, Chun Liu, Xueshi Xin, Wenhe Jia, and Songcen Xu. Renovating parsing r-cnn for accurate multiple human parsing. In *Proc. ECCV*, pages 421–437, 2020.
- [21] Shaoqing Ren, Kaiming He, Ross Girshick, and Jian Sun. Faster r-cnn: Towards real-time object detection with region proposal networks. In *Proc. NeurIPS*, pages 91–99, 2015.
- [22] Tsung-Yi Lin, Priya Goyal, Ross Girshick, Kaiming He, and Piotr Dollár. Focal loss for dense object detection. In *Proc. IEEE Conf. ICCV*, pages 2980–2988, 2017.
- [23] Zhi Tian, Chunhua Shen, Hao Chen, and Tong He. Fcos: Fully convolutional one-stage object detection. In *Proc. IEEE Conf. ICCV*, pages 9627–9636, 2019.
- [24] Ke Gong, Xiaodan Liang, Yicheng Li, Yimin Chen, Ming Yang, and Liang Lin. Instance-level human parsing via part grouping network. In *Proc. ECCV*, pages 770–785, 2018.
- [25] Jian Zhao, Jianshu Li, Yu Cheng, Terence Sim, Shuicheng Yan, and Jiashi Feng. Understanding humans in crowded scenes: Deep nested adversarial learning and a new benchmark for multi-human parsing. In *Proc. ACM MM*, pages 792–800, 2018.
- [26] Qixian Zhou, Xiaodan Liang, Ke Gong, and Liang Lin. Adaptive temporal encoding network for video instance-level human parsing. In *Proc. of ACM MM*, pages 1527–1535, 2018.
- [27] Wei Liu, Dragomir Anguelov, Dumitru Erhan, Christian Szegedy, Scott Reed, Cheng-Yang Fu, and Alexander C Berg. Ssd: Single shot multibox detector. In *Proc. ECCV*, pages 21–37, 2016.
- [28] Joseph Redmon and Ali Farhadi. Yolo9000: better, faster, stronger. In *Proc. IEEE Conf. CVPR*, pages 7263–7271, 2017.
- [29] Joseph Redmon and Ali Farhadi. Yolo v3: An incremental improvement. *arXiv preprint arXiv:1804.02767*, 2018.
- [30] Lichao Huang, Yi Yang, Yafeng Deng, and Yinan Yu. Densebox: Unifying landmark localization with end to end object detection. *arXiv preprint arXiv:1509.04874*, 2015.
- [31] Joseph Redmon, Santosh Divvala, Ross Girshick, and Ali Farhadi. You only look once: Unified, real-time object detection. In *Proc. IEEE Conf. CVPR*, pages 779–788, 2016.
- [32] Hei Law and Jia Deng. Cornernet: Detecting objects as paired keypoints. In *Proc. ECCV*, pages 734–750, 2018.
- [33] Xingyi Zhou, Jiacheng Zhuo, and Philipp Krähenbühl. Bottom-up object detection by grouping extreme and center points. In *Proc. IEEE Conf. CVPR*, pages 850–859, 2019.
- [34] Xingyi Zhou, Dequan Wang, and Philipp Krähenbühl. Objects as points. *arXiv preprint arXiv:1904.07850*, 2019.
- [35] Xier Chen, Yanchao Lian, Licheng Jiao, Haoran Wang, YanJie Gao, and Shi Lingling. Supervised edge attention network for accurate image instance segmentation. In *Proc. ECCV*, pages 617–631, 2020.
- [36] Tong Wu, Yuan Hu, Ling Peng, and Ruonan Chen. Improved anchor-free instance segmentation for building extraction from high-resolution remote sensing images. *Remote Sensing*, 12(18):2910, 2020.

- [37] Hao Chen, Kunyang Sun, Zhi Tian, Chunhua Shen, Yongming Huang, and Youliang Yan. Blendmask: Top-down meets bottom-up for instance segmentation. In *Proc. IEEE Conf. CVPR*, pages 8573–8581, 2020.
- [38] Tao Wang, Ning Xu, Kean Chen, and Weiyao Lin. End-to-end video instance segmentation via spatial-temporal graph neural networks. In *Proc. IEEE Conf. ICCV*, pages 10797–10806, 2021.
- [39] Yuxi Li, Ning Xu, Jinlong Peng, John See, and Weiyao Lin. Delving into the cyclic mechanism in semi-supervised video object segmentation. *Advances in Neural Information Processing Systems*, 33:1218–1228, 2020.
- [40] Haoyu He, Jing Zhang, Qiming Zhang, and Dacheng Tao. Grapy-ml: Graph pyramid mutual learning for cross-dataset human parsing. In *Proc. AAAI*, volume 34, pages 10949–10956, 2020.
- [41] Ke Gong, Yiming Gao, Xiaodan Liang, Xiaohui Shen, Meng Wang, and Liang Lin. Graphonomy: Universal human parsing via graph transfer learning. In *Proc. IEEE Conf. CVPR*, pages 7450–7459, 2019.
- [42] Tianfei Zhou, Wenguan Wang, Si Liu, Yi Yang, and Luc Van Gool. Differentiable multi-granularity human representation learning for instance-aware human semantic parsing. In *Proc. IEEE Conf. CVPR*, pages 1622–1631, 2021.
- [43] Tao Ruan, Ting Liu, Zilong Huang, Yunchao Wei, Shikui Wei, and Yao Zhao. Devil in the details: Towards accurate single and multiple human parsing. In *Proc. AAAI*, volume 33, pages 4814–4821, 2019.
- [44] Xinchen Liu, Meng Zhang, Wu Liu, Jingkuan Song, and Tao Mei. Braidnet: Braiding semantics and details for accurate human parsing. In *Proc. ACM MM*, pages 338–346, 2019.
- [45] Ruyi Ji, Dawei Du, Libo Zhang, Longyin Wen, Yanjun Wu, Chen Zhao, Feiyue Huang, and Siwei Lyu. Learning semantic neural tree for human parsing. In *Proc. ECCV*, pages 205–221, 2020.
- [46] Sanyi Zhang, Guo-Jun Qi, Xiaochun Cao, Zhanjie Song, and Jie Zhou. Human parsing with pyramidal gather-excite context. *IEEE Transactions on Circuits and Systems for Video Technology (TCSVT)*, 31(3):1016–1030, 2021.
- [47] Ross Girshick, Ilija Radosavovic, Georgia Gkioxari, Piotr Dollár, and Kaiming He. Detectron. <https://github.com/facebookresearch/detectron>, 2018.
- [48] Peike Li, Yunqiu Xu, Yunchao Wei, and Yi Yang. Self-correction for human parsing. *IEEE Transactions on Pattern Analysis and Machine Intelligence (TPAMI)*, 2021.
- [49] Haifang Qin, Weixiang Hong, Wei Chih Hung, Yi Hsuan Tsai, and Ming Hsuan Yang. A top-down unified framework for instance-level human parsing. In *BMVC*, 2019.
- [50] Ian Goodfellow, Jean Pouget-Abadie, Mehdi Mirza, Bing Xu, David Warde-Farley, Sherjil Ozair, Aaron Courville, and Yoshua Bengio. Generative adversarial nets. In *Proc. NeurIPS*, volume 27, 2014.
- [51] Tsung-Yi Lin, Piotr Dollár, Ross Girshick, Kaiming He, Bharath Hariharan, and Serge Belongie. Feature pyramid networks for object detection. In *Proc. IEEE Conf. CVPR*, pages 2117–2125, 2017.
- [52] Jonathan Long, Evan Shelhamer, and Trevor Darrell. Fully convolutional networks for semantic segmentation. In *Proc. IEEE Conf. CVPR*, pages 3431–3440, 2015.
- [53] Yuhui Yuan, Xilin Chen, and Jingdong Wang. Object-contextual representations for semantic segmentation. In *Proc. ECCV*, pages 173–190, 2020.
- [54] Jiahui Yu, Yuning Jiang, Zhangyang Wang, Zhimin Cao, and Thomas Huang. Unitbox: An advanced object detection network. In *Proc. ACM MM*, pages 516–520, 2016.
- [55] Liang-Chieh Chen, Yukun Zhu, George Papandreou, Florian Schroff, and Hartwig Adam. Encoder-decoder with atrous separable convolution for semantic image segmentation. In *Proc. ECCV*, pages 801–818, 2018.
- [56] Liang-Chieh Chen, George Papandreou, Iasonas Kokkinos, Kevin Murphy, and Alan L Yuille. Deeplab: Semantic image segmentation with deep convolutional nets, atrous convolution, and fully connected crfs. *IEEE Transactions on Pattern Analysis and Machine Intelligence (TPAMI)*, 40(4):834–848, 2017.
- [57] Guo-Jun Qi. Hierarchically gated deep networks for semantic segmentation. In *Proc. IEEE Conf. CVPR*, pages 2267–2275, 2016.
- [58] Wenguan Wang, Hailong Zhu, Jifeng Dai, Yanwei Pang, Jianbing Shen, and Ling Shao. Hierarchical human parsing with typed part-relation reasoning. In *Proc. IEEE Conf. CVPR*, pages 8929–8939, 2020.
- [59] Wenguan Wang, Tianfei Zhou, Siyuan Qi, Jianbing Shen, and Song-Chun Zhu. Hierarchical human semantic parsing with comprehensive part-relation modeling. *IEEE Transactions on Pattern Analysis and Machine Intelligence (TPAMI)*, 2021.
- [60] Xiaolong Wang, Ross Girshick, Abhinav Gupta, and Kaiming He. Non-local neural networks. In *Proc. IEEE Conf. CVPR*, pages 7794–7803, 2018.
- [61] Yuxin Wu and Kaiming He. Group normalization. In *Proc. ECCV*, pages 3–19, 2018.
- [62] Henghui Ding, Xudong Jiang, Ai Qun Liu, Nadia Magnenat Thalmann, and Gang Wang. Boundary-aware feature propagation for scene segmentation. In *Proc. IEEE Conf. ICCV*, pages 6819–6829, 2019.
- [63] Towaki Takikawa, David Acuna, Varun Jampani, and Sanja Fidler. Gated-scnn: Gated shape cnns for semantic segmentation. In *Proc. IEEE Conf. ICCV*, pages 5229–5238, 2019.
- [64] Tsung-Yi Lin, Michael Maire, Serge Belongie, James Hays, Pietro Perona, Deva Ramanan, Piotr Dollár, and C Lawrence Zitnick. Microsoft coco: Common objects in context. In *Proc. ECCV*, pages 740–755, 2014.
- [65] Ziwei Zhang, Chi Su, Liang Zheng, and Xiaodong Xie. Correlating edge, pose with parsing. In *Proc. IEEE Conf. CVPR*, pages 8900–8909, 2020.
- [66] Xiaomei Zhang, Yingying Chen, Bingke Zhu, Jinqiao Wang, and Ming Tang. Part-aware context network for human parsing. In *Proc. IEEE Conf. CVPR*, pages 8971–8980, 2020.
- [67] Maxim Berman, Amal Rannen Triki, and Matthew B Blaschko. The lovász-softmax loss: A tractable surrogate for the optimization of the intersection-over-union measure in neural networks. In *Proc. IEEE Conf. CVPR*, pages 4413–4421, 2018.
- [68] Jia Deng, Wei Dong, Richard Socher, Li-Jia Li, Kai Li, and Li Fei-Fei. Imagenet: A large-scale hierarchical image database. In *Proc. IEEE Conf. CVPR*, pages 248–255, 2009.
- [69] Jiانشu Li, Jian Zhao, Yunchao Wei, Congyan Lang, Yidong Li, Terence Sim, Shuicheng Yan, and Jiashi Feng. Multiple-human parsing in the wild. *arXiv preprint arXiv:1705.07206*, 2017.
- [70] Xizhou Zhu, Yuwen Xiong, Jifeng Dai, Lu Yuan, and Yichen Wei. Deep feature flow for video recognition. In *Proc. IEEE Conf. CVPR*, pages 2349–2358, 2017.
- [71] Xizhou Zhu, Yujie Wang, Jifeng Dai, Lu Yuan, and Yichen Wei. Flow-guided feature aggregation for video object detection. In *Proc. IEEE Conf. ICCV*, pages 408–417, 2017.
- [72] Hengshuang Zhao, Jianping Shi, Xiaojuan Qi, Xiaogang Wang, and Jiaya Jia. Pyramid scene parsing network. In *Proc. IEEE Conf. CVPR*, pages 2881–2890, 2017.
- [73] Liulei Li, Tianfei Zhou, Wenguan Wang, Jianwu Li, and Yi Yang. Deep hierarchical semantic segmentation. In *Proc. IEEE Conf. CVPR*, 2022.
- [74] Wenguan Wang, Zhijie Zhang, Siyuan Qi, Jianbing Shen, Yanwei Pang, and Ling Shao. Learning compositional neural information fusion for human parsing. In *Proc. IEEE Conf. ICCV*, pages 5703–5713, 2019.